



ECOLOGICAL SOCIETY OF AMERICA

Ecology/Ecological Monographs/Ecological Applications

PREPRINT

This preprint is a PDF of a manuscript that has been accepted for publication in an ESA journal. It is the final version that was uploaded and approved by the author(s). While the paper has been through the usual rigorous peer review process of ESA journals, it has not been copy-edited, nor have the graphics and tables been modified for final publication. Also note that the paper may refer to online Appendices and/or Supplements that are not yet available. We have posted this preliminary version of the manuscript online in the interest of making the scientific findings available for distribution and citation as quickly as possible following acceptance. However, readers should be aware that the final, published version will look different from this version and may also have some differences in content.

The doi for this manuscript and the correct format for citing the paper are given at the top of the online (html) abstract.

Once the final published version of this paper is posted online, it will replace the preliminary version at the specified doi.

1 LINKS BETWEEN DEEP-SEA RESPIRATION AND COMMUNITY DYNAMICS

2

3 Henry A. Ruhl^{1*}, Brian J. Bett¹, Sarah J.M. Hughes², Claudia H.S. Alt², Elizabeth J. Ross²,
4 Richard S. Lampitt¹, Corinne A. Pebody¹, Kenneth L. Smith³, and David S.M. Billett¹

5

6 ¹National Oceanography Centre, University of Southampton Waterfront Campus, European
7 Way, Southampton SO14 3ZH, UK

8

9 ²School of Ocean and Earth Science, University of Southampton, National Oceanography
10 Centre, European Way, Southampton, SO14 3HZ, UK

11

12 ³Monterey Bay Aquarium Research Institute, 7700 Sandholdt Road, Moss Landing, CA 95039,
13 USA

14

15 * E-mail: h.ruhl@noc.ac.uk

16

17

preprint

18 **Abstract**

19 It has been challenging to establish the mechanisms that link ecosystem functioning to
 20 environmental and resource variation, as well as community structure, composition and
 21 compensatory dynamics. A compelling hypothesis of compensatory dynamics, known as ‘zero-
 22 sum’ dynamics, is framed in terms of energy resource and demand units, where there is an
 23 inverse link between the number of individuals in a community and the mean individual
 24 metabolic rate. However, body-size energy distributions that are non-uniform suggest a niche
 25 advantage at a particular size class, which suggests a limit to which metabolism can explain
 26 community structuring. Since 1989, the composition and structure of abyssal seafloor
 27 communities in the northeast Pacific and northeast Atlantic have varied inter-annually with links
 28 to climate and resource variation. Here, for the first time, class and mass-specific individual
 29 respiration rates were examined along with resource supply and time series of density and
 30 biomass data of the dominant abyssal megafauna, echinoderms. Both sites had inverse
 31 relationships between density and mean individual metabolic rate. We found fourfold variation
 32 in echinoderm respiration over inter-annual timescales at both sites, which were linked to shifts
 33 in species composition and structure. In the north-eastern Pacific, the respiration of mobile
 34 surface deposit feeding echinoderms was positively linked to climate-driven particulate organic
 35 carbon fluxes with a temporal lag of about one year, respiring about 1-6% of the annual
 36 particulate organic carbon flux.

37 **Keywords:** compensatory dynamics, zero-sum dynamics, respiration, biogeochemistry, carbon,
 38 benthic, deep sea, echinoderm

39

40 **Introduction**

41 In recent decades, long-term trends in ocean environmental variables have been identified
 42 including warming, acidification, and productivity (Orr et al. 2005, Gehlen et al. 2007, Frölicher
 43 et al. 2009, Keeling et al. 2010, Steinacher et al. 2010). Understanding the relationships between
 44 environmental drivers and ecological variation over time in the deep sea comes from relatively
 45 few records (Glover et al. 2010, Ruhl et al. 2011). Links have been found between climate-
 46 driven shifts in sea surface productivity, sinking particulate organic carbon (POC) flux and deep-
 47 sea biomass, density, and community composition over periods as short as months (Ruhl et al.
 48 2008, Smith et al. 2008, Billett et al. 2010, Moeseneder et al. 2012). Nevertheless, improving
 49 estimates of how the structural and functional attributes of benthic deep-sea systems will respond
 50 to a changing climate require improved understanding of ecological mechanisms and
 51 biogeochemical processes.

52 Assemblages of benthic megafauna at Station M (Sta. M) in the northeast Pacific and the
 53 Porcupine Abyssal Plain (PAP) in the northeast Atlantic have undergone substantial changes in
 54 their abundance and composition at the seafloor since 1989 (Billett et al. 2010, Ruhl 2008).
 55 Echinoderms dominate the mobile benthic megafauna (i.e. for marine benthic fauna this includes
 56 those with mass of about 1g wet weight or more) at these sites (Billett et al. 2010, Ruhl 2008).
 57 The marked dynamics provided an opportunity to investigate mechanisms that may relate to
 58 changes in composition and structure, and their connection to biogeochemical processes and
 59 ecosystem functions.

60 One of the key sets of mechanisms that are thought to control community dynamics are
 61 those relating to compensatory dynamics and resource limitation. The hypothesis of
 62 ‘compensatory dynamics’ posits that when resource levels are fixed, total abundance is constant,
 63 and increases in abundance of one taxon are compensated for by reductions in another (Hubbell

64 2001, Ernest and Brown 2001, Houlahan et al. 2007). In real systems, however, evidence for
 65 such interspecific compensatory dynamics of abundances is limited. Specifically, little evidence
 66 exists for >50% negative covariance of abundance between various taxa expected from random
 67 interactions (e.g. Houlahan et al. 2007). Indeed, interspecific compensation can occur without
 68 negative density covariance, such as when all species might increase in abundance in response to
 69 a resource increase, but change their relative rank dominance because of differential resource
 70 use, or when taxa of different size change abundance relative to each other where there is an
 71 inverse relationship between density and mean individual metabolic rate during different parts of
 72 a timeseries.

73 ‘Zero-sum’ dynamics posits a compensation hypothesis that directly examines energetic
 74 compensation (e.g. Ernest et al. 2008, 2009). Respiration is a key measure to frame ecological
 75 variations in a currency that accounts for the fact that resource use rates are dependent, in part,
 76 on body size, where larger fauna have lower mass-specific respiration rates than smaller fauna. A
 77 testable hypothesis of zero-sum theory is that given a fixed resource input and constant
 78 temperature, the total number of individuals (N) in a community is inversely related to the mean
 79 individual metabolic rate (B), where $N \propto B^{-1}$ (Fig. 1). Such an inverse relationship was observed
 80 in, for example, tropical forest data (Ernest et al. 2009). It follows from that hypothesis that if
 81 resources increase (i.e. $[R]/B \propto N$, where R is available resource), that would allow an increase in
 82 density at a given mean individual respiration rate (or any combination of increased density and
 83 mean individual metabolic rate that equates to the increased resource). Fluctuations in resources
 84 over time could thus manifest as residuals from a best fit relationship of the whole time period
 85 where positive residuals relate to increased resource levels (Fig. 1).

86 In a related thread of ecological theory, rank-abundance distributions (RADs) are
 87 believed to be an indicator of biodiversity that describes the abundance and dominance of each
 88 taxa relative to the others and is indicative of resource use by each rank (Motomura 1932,
 89 MacArthur 1957, Whittaker 1965, Sugihara et al. 2003, Thibault et al. 2004). Another
 90 consequence of zero-sum dynamics is that as communities shifted to lower mean individual
 91 respiration rates (more smaller individuals), there would tend to be an increase in relative
 92 dominance of the smaller individuals and decrease in evenness (Fig. 1). Thus, examination of
 93 rank-energy demand distributions provides a more direct measure of resource partitioning than
 94 abundance measures by also accounting for such allometric scaling.

95 Substantial challenges remain in reconciling such strictly size based theories with niche
 96 theories that necessitate other life history traits such as food selectivity differences at a given
 97 body size. A strictly energetic view of community structuring suggests a uniform relationship
 98 between mean individual size and the resources used at each size class. However, multimodal
 99 distributions have been found in body-size energy distributions suggesting a limit to which body
 100 size can explain community structuring (e.g. Ernest 2005), whereby some specific sizes may
 101 have niche advantages in a given habitat.

102 How variation in the structure of echinoderm assemblages influences their net functional
 103 role is poorly understood. One of the key ecosystem functions of benthic fauna is to remineralise
 104 POC that sinks to the seafloor (food supply) through the processes of respiration and nutrient
 105 regeneration. Dynamics of sediment community oxygen consumption (SCOC) is an indicator of
 106 the temporal variation in food demand. However, because of the nature of the respiration
 107 chambers typically used for studying SCOC, the respiratory demands of megafauna assemblages
 108 previously have not been systematically measured in examining food supply and demand.

109 Here we present the first assessment of long-term variation in the respiration of
 110 echinoderm assemblages from deep-sea habitats to provide insights into the mechanisms driving
 111 their structure, dynamics and biogeochemical function. We examined if total respiration of the
 112 echinoderm assemblage is correlated with indicators of community composition and structure
 113 (CCS). We tested predictions of related hypotheses of compensatory dynamics (CD), zero-sum
 114 dynamics (ZSD), and multimodal distribution (MMD) in explaining patterns of assemblage
 115 structure, dynamics and functional role:

116 CD: With no long-term trend in food (resource) levels over time, the sign of covariance
 117 between pairs of taxon-specific respiration is, on average, more negative than positive among all
 118 pairwise combinations;

119 ZSD₁: Mean individual respiration rate is inversely related to total density while mean
 120 individual respiration rate is positively related to evenness of the echinoderm assemblage;

121 ZSD₂: Net respiration of the echinoderm assemblage is positively correlated with
 122 temporal variation in food supply;

123 ZSD₃: Residuals in a regression between mean individual respiration rate and total
 124 echinoderm density are positively related to resource availability; and

125 MMD: Multimodal distributions are present in distributions of energy use across body
 126 sizes.

127 The assemblage was also quantified in terms of food supply and demand, feeding
 128 behavior, and the contribution to remineralisation of organic carbon on the deep seafloor.

129

130

131

132 **Methods**

133 This study combined data from several previously published studies including data from
 134 benthic trawling, analyses of feeding guilds, photographic transects of the seafloor, relationships
 135 between individual body size and respiration rates and POC flux data from *in situ* sediment trap
 136 measurements. We calculated respiratory demand of the echinoderm assemblage for the two
 137 abyssal echinoderm communities by multiplying mass- and class-specific respiration rates by
 138 mean individual biomass and observed density (individuals per unit area) for each taxon during
 139 each observation time. We have built on a body of work that has examined relationships between
 140 individual taxa, their body size, and their respiration rates to make initial estimations of
 141 respiration for larger fauna at the seafloor (Smith 1983, Pipenburg and Schmid 1996, Ambrose et
 142 al. 2001, Rowe et al. 2008). The relationships between individual size and respiration were
 143 determined for each echinoderm class based on a meta-analysis of all available *in situ* respiration
 144 measurements of echinoderms (Hughes et al. 2011), which covered a range of depths to more
 145 than 4000 m depth. We applied a temperature correction for each site modifying the equations
 146 presented in Hughes et al. (2011) so that the PAP temperature correction was set to 2.6°C and
 147 Sta. M to 1.5°C, the measured ambient temperatures at each site. The mass-specific respiration
 148 rate equations take the following form: individual respiration rate = aM^b , where M is individual
 149 wet-weight mass, a is the class specific y-intercept and b is the related exponent.

150

151 *Megafauna sampling*

152 Methods varied according to the specific assemblage examined. Camera sled tows were
 153 conducted at Station M, which is located offshore of the California coastline in the north-eastern
 154 Pacific at 34°50'N, 123°00'W, at about 4100 m depth. Faunal density and body size estimates

155 were determined using photogrammetric techniques on towed camera sled images. The camera
 156 was positioned about 82 cm above the seafloor and operated to create a roughly continuous set of
 157 seafloor images. Here we use a standard definition of megafauna, those fauna identifiable in
 158 these seafloor images (typically ≥ 1 cm in size *sensu* Grassle 1975). The top ten dominant mobile
 159 organisms were enumerated including the Holothuroids *Elpidia* sp., *Peniagone vitrea*, *P.*
 160 *diaphana*, *Scotoplanes globosa*, *Oneirophanta mutabilis*, *Psychropotes longicauda*,
 161 *Abyssocucumis abyssorum* and *Synallactes* sp., the echinoid *Echinocrepis rostrata*, and the
 162 Ophiuroidea, all of which are echinoderms. Echinoderms make up more than 99% of the mobile
 163 individuals observed during the surveys (see Ruhl 2007 for more quantitative details). The
 164 species-specific density and body size data captured from the images was combined with length
 165 to wet weight conversions to calculate biomass. The length to weight conversions originated
 166 from PAP samples using the same species or closest congener in terms of body shape.

167 Benthic trawling was conducted at the Porcupine Abyssal Plain in the vicinity of
 168 48°50'N, 16° 30'W in the north-eastern Atlantic at a depth of about 4850 m. Here megafauna are
 169 those caught in a semi-balloon otter trawl system with an 8.6 m opening and 13 mm stretch mesh
 170 liner in the cod end (Billett et al. 2001, Merrett and Marshall 1981). This system was typically
 171 trawled at about 0.75 m s⁻¹ over the seafloor. Density and biomass data from multiple trawls
 172 during a single cruise were averaged to create monthly values. At this site we only examined the
 173 data for the echinoderms, which made up about 95% of the total trawled biomass (see Billett et
 174 al. 2010 for more quantitative details). We assigned the echinoderm taxa into feeding guilds
 175 based on results from a previous study that examined relative isotope quantities in tissues to
 176 establish the trophic position among a large proportion of the fauna collected in PAP trawls (Iken
 177 et al. 2001). The guilds were delineated as surface deposit feeders (SDF), sub-surface deposit

178 feeders (SSDF), and suspension feeders (SF), and predators/scavengers (P/S). Here too the fauna
 179 were dominated by Holothuroidea including *Amperima rosea*, *O. mutabilis*, *Ellipinion molle*, *Ps.*
 180 *longicauda*, *P. diaphana* (all SDFs) and *Pseudostichopus spp.* (SSDF), as well as Asteroidea
 181 including *Hyphalaster inermis* (SSDF) and *Dytaster grandis grandis* (P/S), Ophiuroidea (SDF),
 182 Echinodea (SDF), and Crinoidea (SF).

183 It is important to note key differences in the methods for density and biomass data for
 184 PAP and Station M. PAP results were based on trawl samples whereas Sta. M were determined
 185 photographically. The Sta. M wet weight biomass was estimated from taxon specific
 186 relationships for length to mass, and only the top ten most abundant mobile epibenthic
 187 megafauna were examined. PAP data quantified four echinoderm feeding guilds, whereas Sta. M
 188 photographic data only quantified animals feeding at the sediment surface. Thus, at Sta. M,
 189 obscured sub-surface deposit feeders are left out of any fauna/function calculations. The trawl
 190 used at PAP substantially under-samples the echinoderms with greater under-sampling likely at
 191 smaller body sizes, but can reproduce variation in key fauna (Bett et al. 2001). For that reason,
 192 only relative variation is considered in conclusions for PAP, rather than the specific values.

193

194 *Community indicators*

195 In order to examine relationships between energetic, biogeochemical and community
 196 variation we used monthly records to derive a series of uni- and multi-variate community
 197 descriptors. These descriptors included total echinoderm abundances in terms of density (TA_D)
 198 and biomass (TA_B), as well as total echinoderm respiration (TR). Also included were indices of
 199 species composition similarity based on density data (SC_D), biomass (SC_B), and energetic
 200 demand (SC_E). We also computed Pielou's evenness (J') from density data, as well as a series of

201 rank-abundance distribution similarity indices based on density (RAD_D), biomass (RAD_B), and
 202 energetic demand (RAD_E), where the taxon identity is replaced by rank during each sampling
 203 time. For the PAP dataset, we also calculated a feeding guild composition index based on energy
 204 use by each guild (FGC_E). These indices were created by $\log(x+1)$ transforming the relevant
 205 data and then calculating the Bray-Curtis similarity between all the pairwise sample times. Then,
 206 for each data type, we used the multidimensional scaling (MDS) x-ordinates plotted over time as
 207 indicators of community variation.

208

209

210 *Biogeochemical fluxes*

211 Food supply at both sites was quantified as POC flux using deep-sea sediment trap
 212 samples at each site using methods described previously (Baldwin et al. 1998, Lampitt et al.
 213 2010). Each trap is conical in shape and collected material sinking through a baffled entrance
 214 with a 0.25 m^{-2} opening. Cups at the bottom of the trap move sequentially to capture samples in
 215 time-series with regular intervals. These samples are then returned to shore and analyzed for
 216 POC content (see Smith et al. 2008 for more quantitative details on Sta. M fluxes). The POC flux
 217 data used for Sta. M are a composite of 50 and 600 mab trap data where gaps in the 600 mab
 218 record are filled with 50 mab data that has had correction to account for the fact that the 50 mab
 219 trap can experience flux of resuspended particulates. This correction was made in the form of a
 220 linear regression between using 50 mab as the explanatory variable for the 600 mab data series.
 221 POC fluxes at PAP at 3000 m depth were measured using conical sediment traps (see Lampitt et
 222 al. 2010 for more quantitative details on fluxes at PAP). However, POC values for the time

223 period October 2008 – July 2011 were estimated from volume flux measurements using an
 224 empirically derived linear relationship between the two variables ($r^2 = 0.75$, $p < 0.0001$).

225

226 *Analytical approach*

227 Correlations between TR and the community indicators (CCS) described above were
 228 tested using the Spearman's rank correlation test (r_s), as well as a similarity matrix correlation
 229 test with randomization based significance testing (R, Clark 1993). Covariances of resource use
 230 (respiration) were also calculated between each taxon pair across sampling times (CD). The
 231 mean individual respiration rate (TR/TA_D) was tested for correlation to total density and
 232 evenness (J') with an F-test used to determine significance for relationships between mean
 233 individual respiration rate and total density and r_s for correlating to evenness (ZSD_1). Correlation
 234 between TR and POC flux (ZSD_2) was tested via r_s . POC flux changes were allowed to precede
 235 TR in cross correlation revealing the time lag with a peak in correlation coefficient. The residuals
 236 of a least squares power function regression of mean individual respiration rate and total density
 237 were then similarly correlated with POC flux via r_s (ZSD_3). The Kolmogorov-Smirnov Test was
 238 used to determine if body size energy distributions were significantly different from a uniform
 239 distribution (MMD).

240 A ratio of food supply to demand was then examined. Here we considered respiration
 241 values in terms of $mg\ C\ m^{-2}\ d^{-1}$ for direct comparison to POC flux units using a respiratory
 242 quotient of 0.85 (Smith 1978). The proportion of monthly TR in terms of food demand (TR_C) to
 243 POC flux ($TR_C:POC\ flux$) provided estimation of the proportion of food input used by the
 244 assemblage where TR_C was compared with the synoptic POC flux, as well as the mean POC flux
 245 from the preceding 12 months.

246

247

248 **Results**

249 ***Station M***

250 The Sta. M time series exhibited variations in TR of about a factor of four (Fig. 2A). The
 251 concentration of sampling with time at Sta. M provides a clear indication that variations in
 252 respiration of the assemblage can have significant shifts at inter-annual scales. For example,
 253 1991 and 1994 have significantly different median respiration rates (Mann-Whitney U-test, $p =$
 254 0.02). Respiration (TR) was significantly correlated with both TA_D and TA_B with respiration
 255 being more highly correlated to TA_B (CCS hypothesis, Table 1). TA_D and TA_B were not directly
 256 correlated. In addition, TR was correlated to the species composition descriptors SC_D , SC_B , and
 257 SC_E (Fig. 2, Table 1).

258 There were also significant correlations between TR and rank abundance indicators
 259 RAD_D , RAD_B , and RAD_E , which were based on density, biomass and energetic demand
 260 respectively (CCS hypothesis, Table 1). Each of these RAD types not only had changes in RAD
 261 shape (i.e. relative dominance and evenness), but there were also major shifts in terms of the
 262 relative ranks of several taxa (Fig 3A). Although RAD_D , RAD_B , and RAD_E variation had
 263 similarities, the taxonomic identity of the dominant taxon was frequently not the same from one
 264 RAD type to the next and many taxa exhibited substantial changes in relative dominance, in
 265 addition to density, biomass and resource use. For example, near the start of the time series in
 266 June 1991, density, biomass, and respiration were each dominated by a different taxon (Fig. 3A,
 267 B and C). There were also major shifts in rank over time at Sta. M, as shown notably by changes
 268 in the holothurian *Elpidia* spp., the urchin *Echinocrepis rostrata*, and the brittle stars

269 Ophiuroidea dominated by *Ophiura bathybia*. Changes in SC_E were most closely correlated with
 270 density variation of these three taxa ($R = 0.58-0.65$, $p < 0.001$).

271 The covariance in TR between taxa over time was about $\frac{1}{2}$ negative in sign considering
 272 all possible taxon-specific pairwise cases (CD hypothesis). There was a significant negative
 273 correlation between mean respiration per individual and total density, an expectation where
 274 increases in density are compensated by lower mean individual respiration rates (ZSD₁
 275 hypothesis; $F = 23.2$, $p < 0.001$; Fig. 4). With no correlation between time and POC flux over the
 276 whole time series, there was no monotonic change in resources observed during the study period.
 277 Evenness was significantly lower when mean individual respiration rate was lower (ZSD₁
 278 hypothesis; $r_s = 0.48$, $p = 0.002$; Fig. 4). A positive correlation was found between TR and POC
 279 flux with a time lag of 13 months (ZSD₂ hypothesis; $r_s = 0.45$, $p = 0.03$) with an intensity and
 280 time lag similar to results for correlations between SC_D and POC flux found previously (Ruhl
 281 2008). The monthly echinoderm assemblage food demand was $\sim 1-6\%$ of the mean POC flux
 282 food supply of the preceding 12 months, and as much as 10% of the synoptic monthly supply
 283 (Fig. 6A). The residuals of the density-mean respiration rate relationship are positively correlated
 284 to monthly POC flux to the seafloor with a time lag of 12 months (ZSD₂ hypothesis; $r_s = 0.42$, p
 285 $= 0.03$; Fig. 4). When body- size energy distributions were examined across these two different
 286 parts of the time series, each period showed multimodal distributions (MMD hypothesis, $p <$
 287 0.001 , Fig. 5).

288

289 **PAP**

290 Here too we found approximately four fold variation in TR (Fig. 2B). The TR variation
 291 was significantly correlated with TA_D , TA_B , SC_D and SC_E , but not significantly to SC_B (CCS

292 hypothesis, Table 1). Correlations were also found between TR and RAD descriptors matching
 293 results for Station M. Similarly, TA_D and TA_B were not correlated at PAP. The two major peaks
 294 in respiration at PAP were associated with a peak in TA_D in 1997 and TA_B in 1998 (Fig. 2D).

295 From the start of the PAP time series, the smaller holothurian *A. rosea* increased in
 296 relative density by several orders of magnitude, as well as rank to become most numerous by
 297 April 1997, but *A. rosea* declined again by the end of the time series (Fig. 3D). The increases in
 298 *A. rosea* were accompanied by a reduction in abundance and rank dominance of the holothurian
 299 *O. mutabilis*. It is notable that in April 1997 the dominant species in terms of biomass (*O.*
 300 *mutabilis*) was not so in terms of resource use. In another example, in April 1999 the most
 301 dominant in terms of density (*A. rosea*) was not so in terms of resource use (Fig. 3D, E and F).
 302 The relatively large holothurian *Psychropotes longicauda* had relatively high dominance in terms
 303 of energetic demand when compared to its dominance by density. *Psychropotes longicauda* also
 304 had the strongest correlation between any taxon-specific density and SC_E among the echinoderms
 305 at PAP ($R = 0.76, p < 0.001$).

306 Respiration (TR) variation was highly correlated to the feeding guild composition in
 307 terms of their energy demand (FGC_E , $R = 0.86, p < 0.001$), where variation in surface deposit
 308 feeder (SDF) explained the greatest proportion of variation in FGC_E . While PAP trawl samples
 309 spanned four feeding guilds described by Iken et al. (2001), variation in FGC_E was most related
 310 to SDF. The SDF guild made up ~87% of the individuals on average, followed in dominance by
 311 sub-surface deposit feeders (SSDF, Fig. 6B) with Fig. 3 indicating guild assignments of the
 312 dominant fauna during relatively contrasting community compositions. Together these two
 313 guilds made up an average of 95-99 % of the echinoderms in the trawl collections for each of the
 314 sampling times, with suspension feeders and predator/scavengers making up the remaining two

315 guilds. The SDF respiration for the time series was more variable than that of the SSDF, which
 316 were relatively stable. However, the ratio of SDF to SSDF was not directly correlated to TR.

317 Covariances between pairwise taxon-specific energy demand over time were also about
 318 $\frac{1}{2}$ negative in sign (CD). Like Sta. M, there was also a significant negative correlation between
 319 mean individual respiration and total density (ZSD₁ hypothesis, $F = 81.5$, $p < 0.001$; Fig. 4), with
 320 higher evenness positively related to mean individual respiration rate ($r_s = 0.80$, $p < 0.001$). At
 321 PAP, TR was not found to increase relative to preceding POC flux by cross correlation analysis
 322 (ZSD_{2 and 3} hypotheses), as was done with Sta. M data, but this result could be related to the
 323 lower temporal resolution in data for PAP. Direct comparisons of POC flux quantity inputs (food
 324 supply) to TR (food demand) at PAP were not possible because of the known fishing efficiency
 325 issue with the otter trawl system.

326
 327 **Discussion**

328 Total respiration (TR) of the echinoderm assemblage was related to community
 329 indicators with biomass based indicators at both sites being more correlated to TR than density
 330 indicators in most cases (CCS hypothesis, Fig. 2, Table 1). Changes in distribution shape are
 331 evident in the rank-abundance distributions (RADs Fig. 3), but also the ranks of the top ten
 332 dominant taxa over time with some taxa changing across ten or more ranks. Changes in taxon
 333 rank between density, biomass and respiration RADs were driven, in part, by the fact that smaller
 334 fauna have higher mass-specific respiration rates than larger fauna. As a result, the apparent
 335 dominance of a particular species in terms of density and/or biomass did not always translate to
 336 that species being dominant in terms of resource use (respiration).

337 Compensatory dynamics in terms of >50% negative covariances were not found, even in
 338 terms of TR (CD hypothesis). Compensation in terms of zero-sum dynamics was, however,
 339 observed at both sites with links to evenness (ZSD₁ hypothesis, Fig. 4.). Here, when fewer
 340 individuals were present, there tended to be higher mean individual respiration rates at both sites.
 341 Differences between sites in density and mean individual respiration relate to the different
 342 sampling tools as discussed in the methods. Zero-sum dynamics have also been found in
 343 communities of desert rodents and in a tropical forest community (White et al. 2004, Ernest et al.
 344 2008, 2009).

345 At Sta. M, where links between food supply and community dynamics are best
 346 understood, we found evidence of the interplay between zero-sum compensation and the non-
 347 steady state forcing of the system by changes in food supply. TR was correlated to POC flux
 348 (ZSD₂ hypothesis), and POC flux appeared to modulate zero-sum relationships between mean
 349 individual respiration rate and total density (ZSD₃ hypothesis). We found that although there
 350 were straightforward metabolism-based zero-sum compensation dynamics like those evident in
 351 Fig. 4, there was also a correlation of POC flux with the residual variation in density found in Fig
 352 4A. Thus, as the density deviates from that expected by zero-sum compensation, food supply can
 353 explain some of this deviation in terms of more food supply relating to positive density residuals
 354 (Fig. 1).

355 Energetic theories of community structuring alone are not sufficient to explain the
 356 multimodal nature of the body size energy distribution at Sta. M (MMD hypothesis, Fig. 5). POC
 357 flux variation can be differentiated into temporal variance, as well as composition in terms of
 358 pigments, lipids and other nutrients. Both quantity and quality of food supply to the benthos vary
 359 over time. This temporal variation in a common set of resources to a community of differentially

360 responding fauna likely provides the mechanism by which the abyssal echinoderms have
 361 exhibited substantial switches in rank abundance (e.g. FitzGeorge-Balfour et al. 2010). The
 362 habitat and its scale may also lend advantage to fauna of particular size classes (Ernest 2005). It
 363 will be informative to continue examination of suitable datasets for MMD patterns, particularly
 364 where there are data that span larger size ranges and assemblage types. However, care must be
 365 taken in considering potential biases from sampling gear (Bett 2013).

366 The degree to which taxon-specific niche vs. size-related mechanisms drive community
 367 dynamics is unclear, but indications of both were evident. Within a food limited system, we
 368 observed compensatory dynamics, rank switches, and non-random links between TR and
 369 measures of biodiversity such as SC_D and evenness. At PAP, where sampling included a broader
 370 range of feeding types, there were indications of correspondence between feeding guild variation
 371 and respiration. Links to resource availability and assemblage changes in terms of density have
 372 been linked to environmental conditions at Station M (Ruhl 2008, Ruhl et al. 2008) and there is
 373 evidence that these differences translate to changes in reproductive potential (Wigham et al.
 374 2003, Ruhl 2007, FitzGeorge-Balfour et al. 2010). It is important to note, though, that swimming
 375 may provide another effective mechanism for abundance variation of some fauna at the study
 376 sites (Rogacheva et al. 2013). Several observed holothurians are capable of swimming and thus
 377 have potential ability for migration in terms of explaining observed variation, particularly
 378 *Peniagone* spp. and *A. rosea*, but the effectiveness of swimming as a migration mechanism is
 379 unknown.

380 The similarities in TR variation at both Sta. M and PAP suggest substantial variation in
 381 assemblage-related carbon cycle processes, at least on site specific and perhaps larger scales. The
 382 results from Sta. M suggest that food supply drives variation in respiration dynamics, in part. The

383 results from Sta. M also suggest a modest increase in shortfall between the supply and demand of
 384 incoming POC flux, as estimates now include data from the echinoderm assemblage. Because
 385 the efficiency with which POC is assimilated into tissue is generally thought to be proportional
 386 to respiration for these taxa (e.g. van Oevelen et al. 2012), the rates of secondary production
 387 from these assemblages likely have similar variation, as would the rates of remineralisation.
 388 Benthic echinoderms have been estimated to contribute to a substantial portion of inorganic C
 389 production globally (up to about 1/4 that of pelagic inorganic C production, Lebrato et al. 2010).
 390 Even though the echinoderm production rates peak at shallower depths than those studied here,
 391 our results suggest the possibility of substantial temporal variation in those rates, which would
 392 likely apply to any area experiencing similar climate-driven variation.

393 Total respiration rates at PAP have notable similarity to estimates from an inverse model
 394 study. van Oevelen et al. (2012) estimated SDF and SSDF respiration as part of a comprehensive
 395 inverse model budgeting of carbon stocks and flows at PAP. Both our study and the model study
 396 use the trawl sampling as inputs to the estimates, but the linear inverse model approach estimates
 397 these flows through balancing a series of equality and inequality equations where some, but not
 398 all flows are known *a priori*, whereas the estimates presented here are relatively empirical. For
 399 the period September 1996 to October 1998, the SDF respiration values measured here were
 400 about 43 % less than those based on inverse methods for that period.

401 The methods here provide the best available estimates for resource use of the studied
 402 fauna, which include empirical class specific rates that do not rely on *a priori* allometric scaling
 403 relationships. A key limitation should be noted, though. The way we were able to apply size
 404 specific respiration rates to density and body size data over time did not allow for the fact that
 405 there could be variations in individual size-specific respiration over time within each taxon.

406 During periods of higher fluxes, when activity is known to be higher from time lapse
 407 photography (Bett et al. 2001, Vardaro et al. 2009), individuals may have elevated respiration
 408 rates not accounted for here. Such changes in individual respiration in response to food input
 409 would likely increase correlation between POC flux and respiration fundamentally. However,
 410 increased respiration related to activity may also shorten the observed time lag in correlations
 411 between POC flux and respiration. Or it might introduce a multi peaked distribution where a
 412 correlation with little or no time lag might be associated with individual metabolic change and
 413 longer-term lagged correlation such as the one found here, which is driven by density and mass
 414 variations in the community.

415 The significant correlations found here have important unexplained variation, for
 416 example between TR and POC flux. Higher-resolution datasets with greater statistical power to
 417 discern food quantity and quality, as well as demand, will likely be needed to make progress in
 418 explaining a greater portion of variation (e.g. Sherman and Smith 2009). Further consideration of
 419 lateral flux of carbon, the flux of larger detrital aggregates and carrion, irregular pulsed POC flux
 420 delivery contributing to a ‘food bank’, is also warranted in helping to constrain food supply
 421 estimates, as well as the local production of biomass via background microbial chemosynthesis
 422 (Robison et a. 2005, Smith et al. 2006, Company et al. 2008, Drazen et al. 2012).

423 The extensive changes in respiration, resource use, remineralisation, and community
 424 structure and composition meet specific assumptions of climate-driven community variation via
 425 niche-based and energetic abundance mechanisms. Climatic variations such as El Niño or the
 426 North Atlantic Oscillation can relate to ocean circulation, surface production, POC fluxes and
 427 ultimately deep-sea assemblages (reviewed in Smith et al. 2009). The observed changes in rank
 428 abundance of the studied assemblage appear to be related to the availability of a multivariate

429 niche space that includes quantity and quality of food supplies. Moreover, the quantitative
 430 relationships identified between respiration and feeding guild have quantitative links to each
 431 other providing evidence that multiple functional changes can be tied to basic changes in
 432 resources. If projected changes in ocean productivity occur (e.g. Steinacher et al. 2010), we
 433 expect that such changes would translate through to pervasive changes in benthic community
 434 structure and function.

435 As presented here, more long-term synoptic studies of the dynamics of resource
 436 availability, taxon specific resource use and ecosystem function over wider ranges of body size
 437 and taxa could help reconcile size- and energy-based theories of community structuring with
 438 niche theories (Issac et al. 2012), as well as resolve imbalances in biogeochemical dynamics. An
 439 improved understanding of these relationships has implications not only for understanding
 440 climate related impacts on the seafloor and other ecosystems, but also for disentangling climate
 441 from other forcing factors such as natural resource extraction.

442
 443 **Acknowledgements**

444 Work at PAP has been supported in part by the European projects HERMES (Hotspot
 445 Ecosystem Research on the Margins of European Seas) and HERMIONE (Hotspot Ecosystem
 446 Research and Man’s Impacts on European Seas), the EuroSITES open ocean observatory
 447 network, and the UK Natural Environment Research Council (NERC) Research Project Oceans
 448 2025. Funding for work at Sta. M has been supported by the National Science Foundation and
 449 the David and Lucile Packard Foundation. Work from Sta. M contributes to the CCE-LTER
 450 (California Current Ecosystem Long-Term Ecology Research) programme funded by the U.S.
 451 National Science Foundation. Thanks to Craig McClain for insightful discussions on

452 macroecology, as well as thoughtful comments from the editor and anonymous reviewers, all of
453 which benefited the manuscript. This work would not be possible without the efforts of a great
454 number of seagoing crew and technical support and research staff who contributed to collecting
455 this data since 1989 including Jacob Ellena, Roberta Baldwin, Ben Boorman and many others.
456 Identification and curation of collected specimens was made possible in part by, the Scripps
457 Institution of Oceanography Benthic Invertebrate Collection, the Smithsonian Institution, and the
458 Discovery Collections, a joint effort of the National Oceanography Centre and Natural History
459 Museum, London.

preprint

460 **References**

- 461
- 462 Ambrose, W. G., et al. 2001. Role of echinoderms in benthic remineralization in the Chukchi
 463 Sea. *Marine Biology* 139: 937-949.
- 464 Baldwin, R. J., R. C. Glatts, and K. L. Smith, Jr. 1998. Particulate matter fluxes into the benthic
 465 boundary layer at a long time-series station in the abyssal NE Pacific: Composition
 466 and fluxes. *Deep-Sea Research II* 45:643-666.
- 467 Bett, B. J. 2013. Characteristic benthic size spectra: potential sampling artefacts. *Marine Ecology*
 468 *Progress Series* 487:1-6.
- 469 Bett, B. J., M. G. Malzone, B. E. Narayanaswamy, and B. D. Wigham. 2001. Temporal
 470 variability in phytodetritus and megabenthic activity at the seabed in the deep
 471 northeast Atlantic. *Progress in Oceanography* 50:349-368.
- 472 Billett, D. S. M., B. J. Bett, W. D. K. Reid, B. Boorman, and I.G. Priede. 2010. Long-term
 473 change in the abyssal NE Atlantic: The '*Amperima* Event' revisited. *Deep-Sea*
 474 *Research II* 57:1406-1417.
- 475 Clarke, K. R. 1993. Non-parametric multivariate analyses of changes in community structure.
 476 *Australian Journal of Ecology* 18:117-143.
- 477 Company, J. B., et al. 2008. Climate Influence on Deep Sea Populations. *PLoS ONE* 3: e1431.
- 478 Drazen, J. C., D. M. Bailey, H. A. Ruhl, and K. L. Smith, Jr. 2012. The Role of Carrion Supply
 479 in the Abundance of Deep-Water Fish off California. *PLoS ONE* 7:
 480 DOI:10.1371/journal.pone.0049332.
- 481 Ernest, S. K. M. 2005. Body size, energy use, and community structure of small mammals.
 482 *Ecology* 86:1407–1413.

- 483 Ernest, S. K. M., J. H. Brown, K. M. Thibault, E. P. White, and J. R. Goheen. 2008. Zero Sum,
 484 the Niche, and Metacommunities: Long-Term Dynamics of Community Assembly.
 485 *American Naturalist* 172:E257–E269.
- 486 Ernest, S. K. M., E. P. White, and J. H. Brown. 2009. Changes in a tropical forest support
 487 metabolic zero-sum dynamics. *Ecology Letters* 12:507–515.
- 488 FitzGeorge-Balfour, T., et al. 2010. Phytopigments as biomarkers of selectivity in abyssal
 489 holothurians, interspecific differences in response to a changing food supply. *Deep-*
 490 *Sea Research II* 57:1418-1428.
- 491 Frölicher, T. L., F. Joos, G. K. Plattner, M. Steinacher, and S. C. Doney. 2009. Natural
 492 variability and anthropogenic trends in oceanic oxygen in a coupled carbon cycle-
 493 climate model ensemble. *Global Biogeochemical Cycles* 23:GB1003,
 494 doi:10.1029/2008GB003316.
- 495 Gehlen, M., et al. 2007. The fate of pelagic CaCO₃ production in a high CO₂ ocean: a model
 496 study. *Biogeosciences* 4:505-519.
- 497 Glover, A. G., et al. 2010. Temporal change in deep-sea benthic ecosystems: a review of the
 498 evidence from recent time-series studies. *Advances in Marine Biology*
 499 58:doi:10.1016/S0065-2881(10)58001-5.
- 500 Grassle, J. F., H. L. Sanders, R. R. Hessler, G. T. Rowe, and T. McLellan. 1975. Pattern and
 501 zonation: a study of the bathyal megafauna using the research submersible Alvin.
 502 *Deep-Sea Research* 22: 457-481.
- 503 Gruber N., et al., 2012. Rapid Progression of Ocean Acidification in the California Current.
 504 *System Science* DOI: 10.1126/science.1216773.

- 505 Houlahan, J. E., et al. 2007. Compensatory dynamics are rare in natural ecological communities.
 506 Proceedings of the National Academy of Sciences of the United States 104:3273-
 507 3277.
- 508 Hubbell, S.P. 2001. The Unified Neutral Theory of Biodiversity and Biogeography. Princeton
 509 Univ Press, Princeton, NJ.
- 510 Hughes, S. J. M., et al. 2011. Deep-sea echinoderm oxygen consumption rates and an interclass
 511 comparison of metabolic rates in Asteroidea, Crinoidea, Echinoidea, Holothuroidea
 512 and Ophiuroidea. Journal of Experimental Biology 214:2512-2521
- 513 Iken K., T. Brey, U. Wand, I. Voigt, and P. Junghans. 2001. Food web structure of the benthic
 514 community at Porcupine Abyssal Plain (N. Atlantic): a stable isotope analysis.
 515 Progress in Oceanography 50:383-405.
- 516 Isaac, N. J. B., D. Storch, and C. Carbone. 2013. The paradox of energy equivalence Global
 517 Ecology and Biogeography. Global Ecology and Biogeography 22:1–5.
- 518 Keeling, R. F., A. Kortzinger, and N. Gruber. 2010. Ocean deoxygenation in a warming world.
 519 Annual Review of Marine Science 2, doi:10.1146/annurev.marine.010908.163855.
- 520 Lampitt, R. S., I. Salter, B. A. de Cuevas, S. Hartman, K. E. Larkin, and C. A. Pebody, 2010.
 521 Long-term variability of downward particle flux in the deep northeast Atlantic:
 522 Causes and trends. Deep-Sea Research II 57:1346-1361.
- 523 Lauerman, L. M. L., R. S. Kaufmann, and K. L. Smith, Jr. 1996. Distribution and abundance of
 524 epibenthic megafauna at a long time-series station in the abyssal northeast Pacific.
 525 Deep-Sea Research I 43:1075-1104.
- 526 Lebrato, M., et al. 2010. Global contribution of echinoderms to the marine carbon cycle: CaCO₃
 527 budget and benthic compartments. Ecological Monographs 80: 441-467.

- 528 MacArthur, R. H. 1957. On the relative abundance of bird species. Proceedings of the National
 529 Academy of Sciences of the United States 43:293-295.
- 530 Merrett, N. R., and N. B. Marshall. 1981. Observations on the ecology of deep-sea bottom-living
 531 fishes collected off northwest Africa (08°-27° N). Progress in Oceanography 9:185-
 532 244.
- 533 Moeseneder, M. M., K. L. Smith, Jr., H. A. Ruhl, D. O. B. Jones, U. Witte, J. I. Prosser. 2012.
 534 Temporal and depth-related differences in prokaryotic communities in abyssal
 535 sediments associated with particulate organic carbon flux. Deep-Sea Research I
 536 70:26–35.
- 537 Orr, J.C., et al. 2005. Anthropogenic ocean acidification over the twenty-first century and its
 538 impact on calcifying organisms. Nature 437:681-686.
- 539 Piepenburg, D., and M. K. Schmid. 1996. Distribution, abundance, biomass, and mineralization
 540 potential of the epibenthic megafauna of the Northeast Greenland shelf. Marine
 541 Biology 125:321-332.
- 542 Robison, B. H., K. R. Reisnechler, and R. E. Sherlock. 2005. Giant larvacean houses: Rapid
 543 carbon transport to the deep sea floor. Science 308:1609-1611.
- 544 Rogacheva, A., Gebruk A., and C. H. S. Alt. 2013. Holothuroidea of the Charlie Gibbs Fracture
 545 Zone area, northern Mid-Atlantic Ridge. Marine Biology Research 9:587-623.
- 546 Rowe, G. T., et al. 2008. Comparative biomass structure and estimated carbon flow in food webs
 547 in the deep Gulf of Mexico. Deep-Sea Research II 55:2699-2711.
- 548 Ruhl, H.A. 2007. Abundance and size distribution dynamics of abyssal epibenthic megafauna in
 549 the northeast Pacific. Ecology 88:1250-1262.

- 550 Ruhl, H. A. 2008. Community change in the variable resource habitat of the abyssal northeast
 551 Pacific. *Ecology* 89:991-1000.
- 552 Ruhl, H. A., J. A. Ellena, and K. L. Smith, Jr. 2008. Connections between climate, food
 553 limitation, and carbon cycling in abyssal sediment communities. *Proceedings of the*
 554 *National Academy of Sciences of the United States* 105:17006-17011.
- 555 Ruhl, H. A., et al. 2011. Societal need for improved understanding of climate change,
 556 anthropogenic impacts, and geo-hazard warning drive development of ocean
 557 observatories in European Seas. *Progress in Oceanography* 91:1-33.
- 558 Sherman, A. D., and K. L. Smith, Jr. 2009. Deep-sea benthic boundary layer communities and
 559 food supply: A long-term monitoring strategy. *Deep-Sea Res. II* 56:1754-1762.
- 560 Smith, C. R., S. Mincks, and D.J. DeMaster. 2006. A synthesis of benthic-pelagic coupling on the
 561 Antarctic shelf: Food banks, ecosystem inertia and global climate. *Deep-Sea*
 562 *Research II* 53:875-894.
- 563 Smith, Jr, K.L. 1983. Metabolism of 2 dominant epibenthic echinoderms measured at bathyal
 564 depths in the Santa-Catalina Basin. *Marine Biology* 72:249-256.
- 565 Smith, Jr, K. L., and R. S. Kaufmann 1999. Long-term discrepancy between food supply and
 566 demand in the deep eastern North Atlantic. *Science* 284:1174-1177.
- 567 Smith, Jr., K.L., H. A. Ruhl, B. J. Bett, D. S. M. Billett, R. S. Lampitt, and R. S. Kaufmann.
 568 2009. Climate and deep-sea communities, *Proceedings of the National Academy of*
 569 *Sciences of the United States* 46:19211-19218.
- 570 Smith Jr, K.L., H. A. Ruhl, R. S. Kaufmann, and M. Kahru. 2008. Tracing abyssal food supply
 571 back to upper-ocean processes over a 17-year time series in the northeast Pacific.
 572 *Limnology and Oceanography* 53:2655-2667.

- 573 Steinacher M., et al. 2010. Projected 21st century decrease in marine productivity: a multi-model
 574 analysis. *Biogeosciences* 7:979-1005.
- 575 Sugihara, G., L.-F. Bersier, T. R. S. Southwood, L. Pimm, and R. M. May. 2003. Predicted
 576 correspondence between species abundances and dendrograms of niche similarities.
 577 *Proceedings of the National Academy of Sciences of the United States* 100:5246-
 578 5251.
- 579 Thibault, K. M., E. P. White, and S. K. M. Ernest. 2004. Temporal dynamics in the structure and
 580 composition of a desert rodent community. *Ecology* 85:2649-2655.
- 581 van Oevelen, D., K. Soetaert, and C. Heip. 2012. Carbon flows in the benthic food web of the
 582 Porcupine Abyssal Plain: The (un)importance of labile detritus in supporting
 583 microbial and faunal carbon demands. *Limnology and Oceanography* 57:645-664
- 584 Vardaro, M. F., H. A. Ruhl, and K. L. Smith Jr, 2009. Climate variation, carbon flux and
 585 bioturbation in the abyssal North Pacific. *Limnology and Oceanography* 54:2081-
 586 2088.
- 587 White, E. P., S. K. M. Ernest, and K. M. Thibault. 2004. Trade-offs in community properties
 588 through time in a desert rodent community. *American Naturalist* 164:670–676.
- 589 Whittaker, R. H. 1965. Dominance and diversity in land plant communities. *Science* 147:250-
 590 260.
- 591 Wigham, B. D., P. A. Tyler, and D. S. M. Billett. 2003. Reproductive biology of the abyssal
 592 holothurian *Amperima rosea*: an opportunistic response to variable flux in surface
 593 derived organic matter? *Journal of the Marine Biological Association of the United*
 594 *Kingdom* 3:175-188.
- 595

596 Table 1. Statistical correlation results comparing total echinoderm megafauna respiration (TR,
 597 i.e, energy or food demand) from the Sta. M photographic data and PAP trawl data to various
 598 other uni- and multi-variate community descriptors.

Community descriptor	Sta. M (n=37)		PAP (n=15)	
	TR		TR	
univariate	r_s	p	r_s	p
Total abundance as density - TA _D	0.64	<0.001	0.61	0.02
Total abundance as biomass - TA _B	0.82	<0.001	0.94	<0.001
multivariate	R	p	R	p
Species composition similarity from density - SC _D	0.11	0.032	0.34	0.007
Species composition similarity from biomass - SC _B	0.35	<0.001	0.20	0.07
Species composition similarity from energetic demand - SC _E	0.35	<0.001	0.42	0.02
Rank-abundance distribution similarity from density - RAD _D	0.23	<0.001	0.37	0.004
Rank-abundance distribution similarity from biomass - RAD _B	0.58	<0.001	0.49	<0.001
Rank-abundance distribution similarity from energetic demand - RAD _E	0.76	<0.001	0.78	<0.001

599

600 Figure Legends

601 Figure 1. Conceptual model illustrating relationships between mean individual respiration rates
 602 and total density (blue line), as well as and Pielou's evenness index (j' , black line) with arrows
 603 indicating increases in variable quantity. Thus, this theoretical formulation, including residuals,
 604 allows for analysis of data from a temporally dynamic study area.

605
 606 Figure 2. Time series (by month) of echinoderm megafauna community dynamics for the Sta. M
 607 and PAP with: A and B) total respiration of the echinoderm megafauna (\bullet , TR) and an index of
 608 echinoderm species composition similarity based on energetic demand (\circ , SC_E); and C and D)
 609 total density (\bullet , TA_D), total biomass (\circ , TA_B); E and F) Monthly POC flux to 4050 and 3000 m
 610 depth at Sta. M and PAP, respectively. The figure illustrates, in part, that TR varies by up to 4-
 611 fold for each site with some synchrony to community composition.

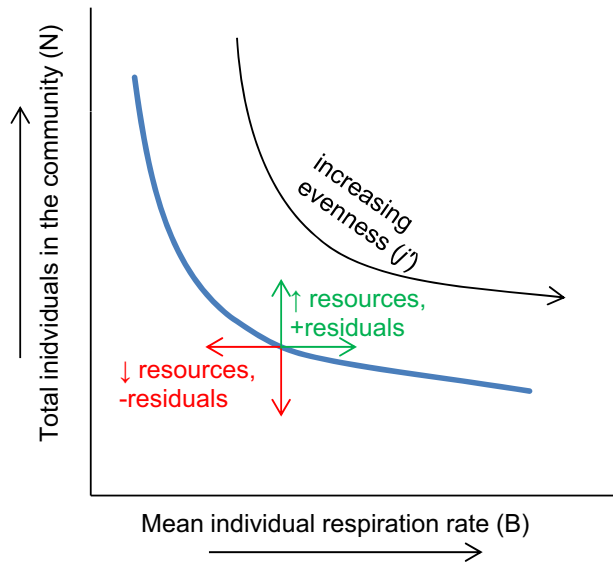
612
 613 Figure 3. Rank distribution plots for Sta. M data for selected times during the time series based
 614 on A) density; B) biomass; and C) energetic demand (respiration). PAP data are similarly shown
 615 in D) for density; E) biomass; and F) energetic demand (respiration). The surface deposit feeders
 616 (SDF) are open bars, sub-surface deposit feeders (SSDF) diagonally hatched bars, suspension
 617 feeders (SF) have horizontally hatched bars, and predators/scavengers (P/S) are cross hatched.
 618 The figure illustrates differences between density, biomass and resource use by species, as well
 619 as how various taxon rank in these factors at specific times, as well as changes in the shape and
 620 magnitude of the RADs.

621

622 Figure 4. Relationship between total density (TA_D), mean individual respiration rates and
 623 Pielou's index of evenness (J') at Sta. M (A) and PAP (B). Points are monthly estimates. This
 624 figure provides data supporting hypothetical relationships presented in Fig. 1. The color in the
 625 points is indicates corresponding evenness with the values provided in the legend to the right of
 626 panel B.

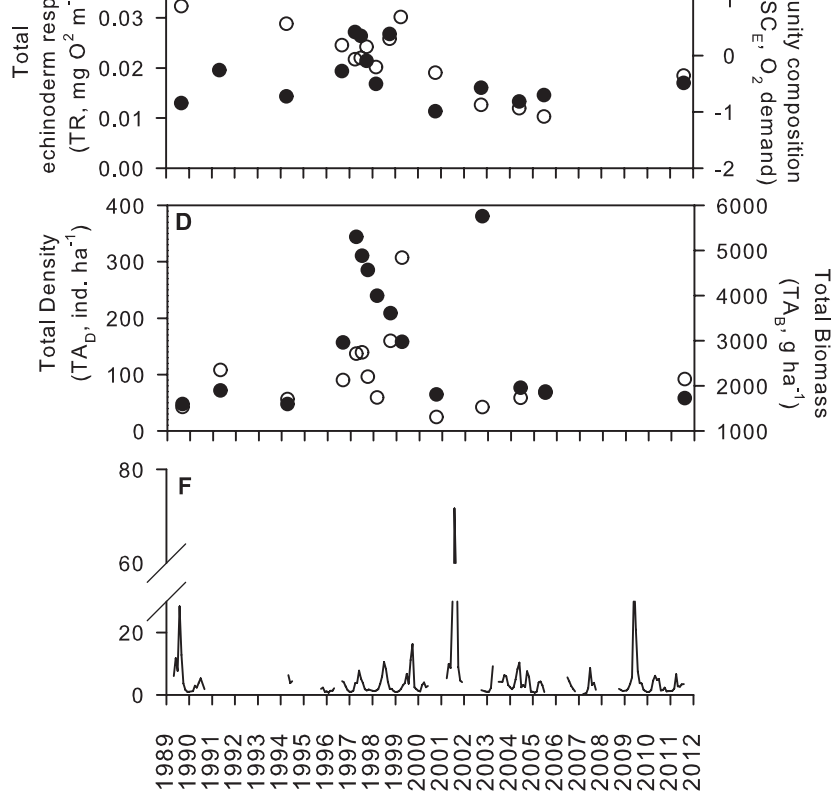
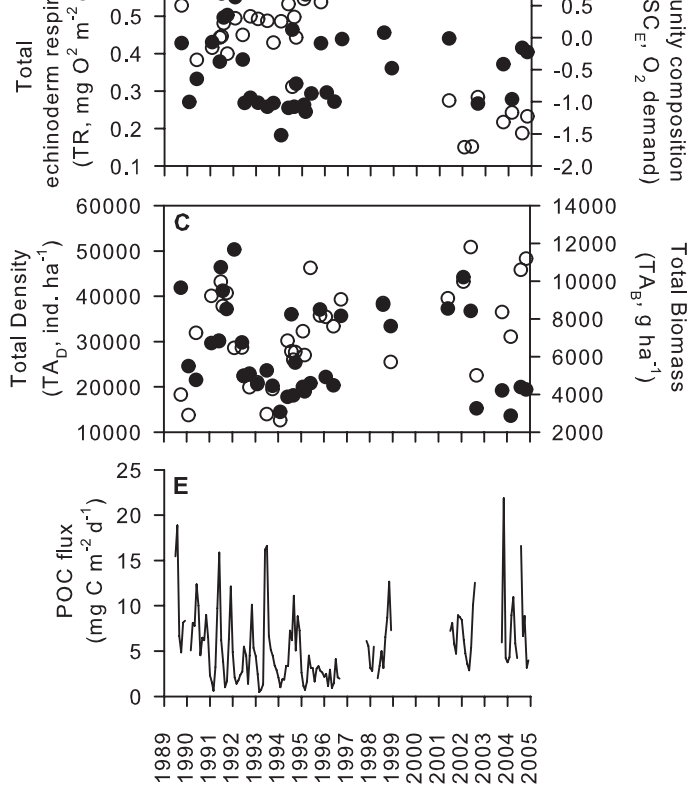
627
 628 Figure 5. Multimodal distributions of total respiration rates in 0.2 log unit size classes at Sta. M
 629 for the two periods with the most different species composition. The total respiration is corrected
 630 for the number of months with data for each period ($n = 29$ for 1989-1998, $n = 8$ for 2001-2004).
 631 This figure illustrates that the assemblage does not have a uniform body-size energy distribution.

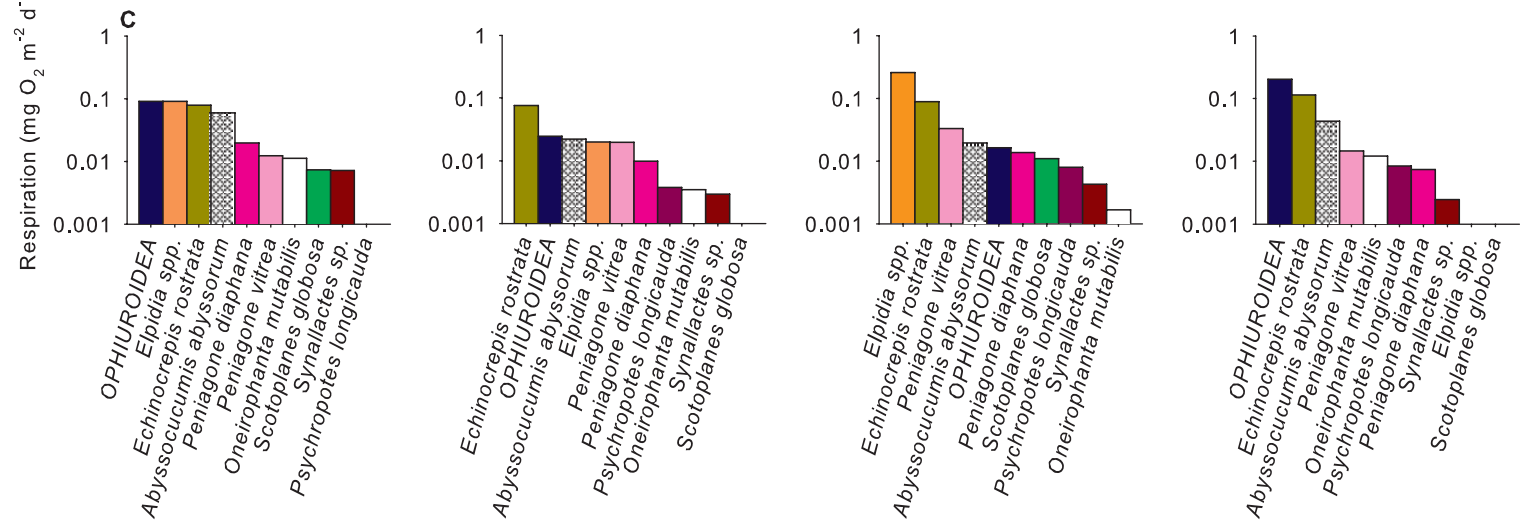
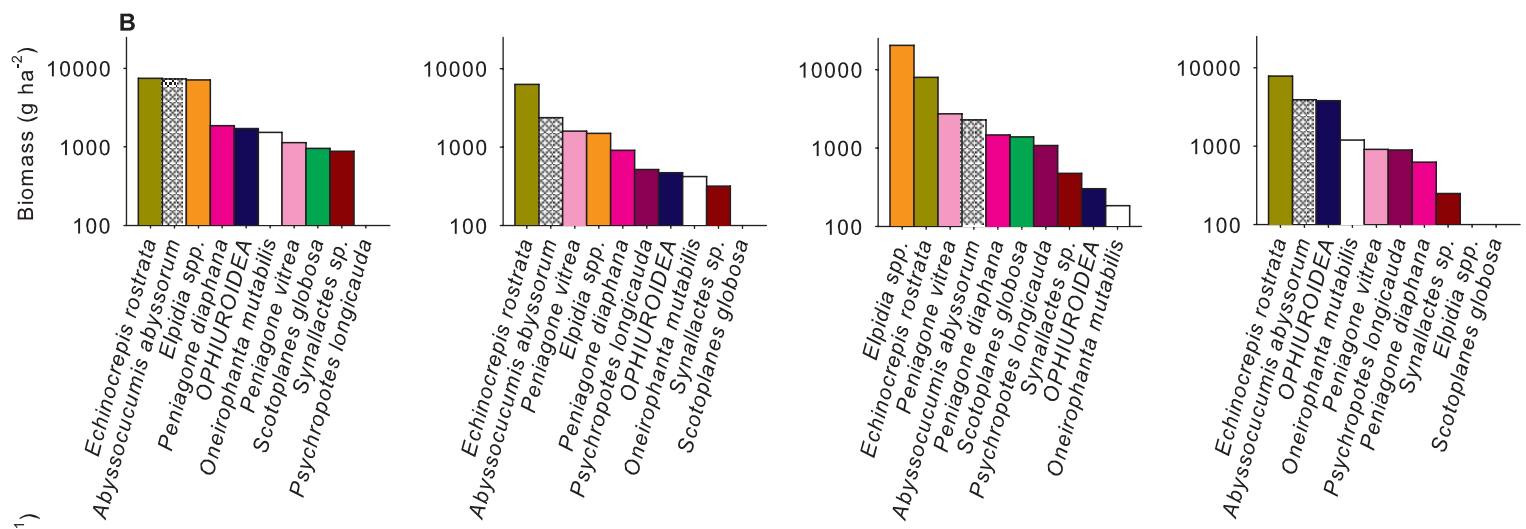
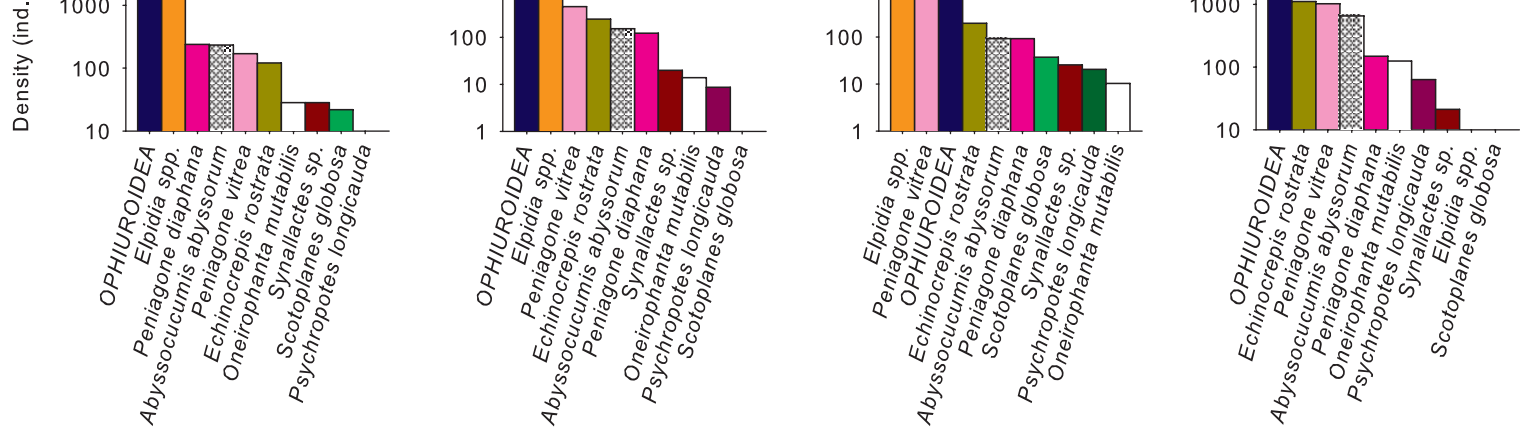
632
 633 Figure 6. Indicators of ecosystem function variation including A) Sta. M time series of monthly
 634 ratio between total echinoderm assemblage respiration in terms of respired C (TR_C) and mean
 635 POC food supplies both for synoptic fluxes ($\circ TR_C$:POC flux) and for the mean of the 12 months
 636 leading up to and including the monthly TR value (\bullet); and B) Monthly energetic demand
 637 estimates for PAP surface deposit feeders (\bullet , SDF) and subsurface deposit feeders (\circ , SSDF), as
 638 well as an index of feeding guild composition over time based on energetic respiratory demand
 639 (\times , FGC_E).

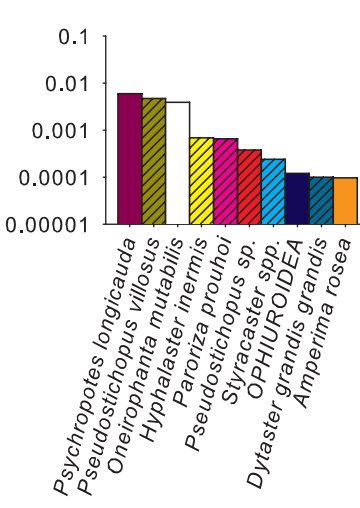
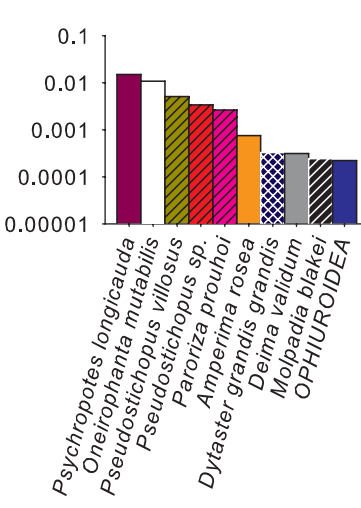
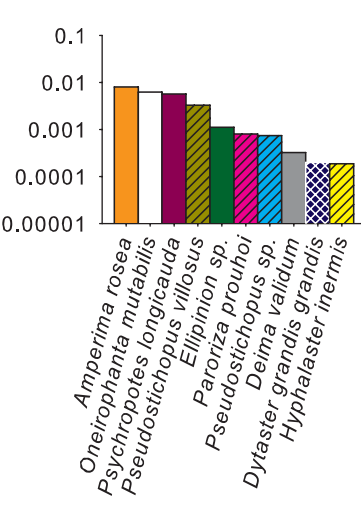
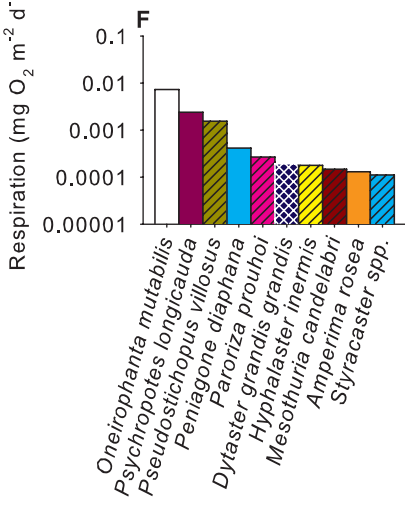
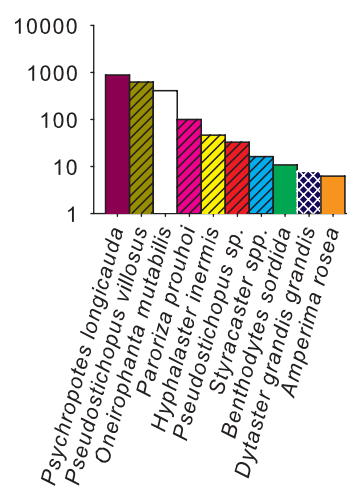
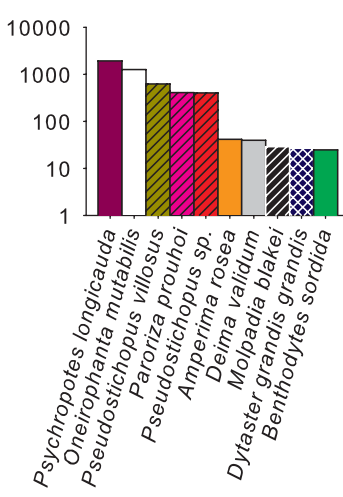
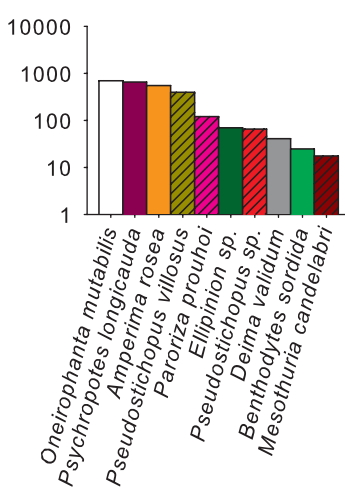
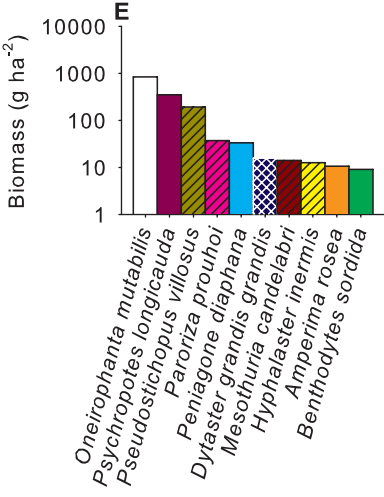
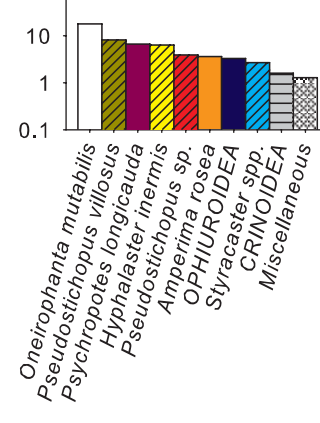
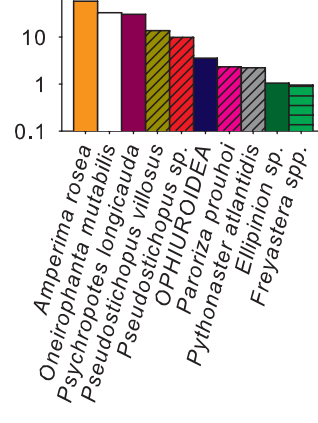
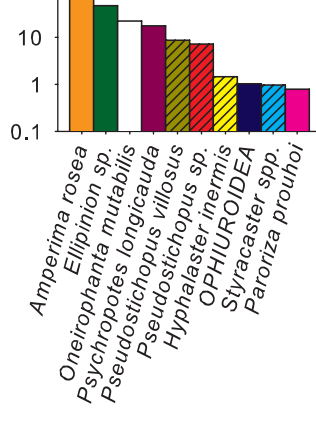
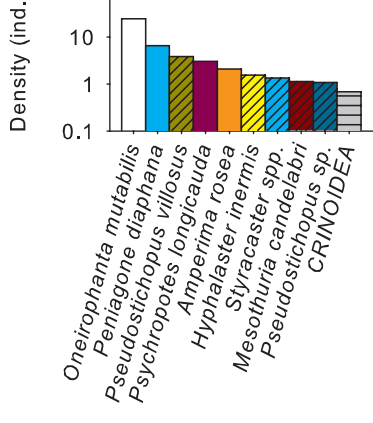


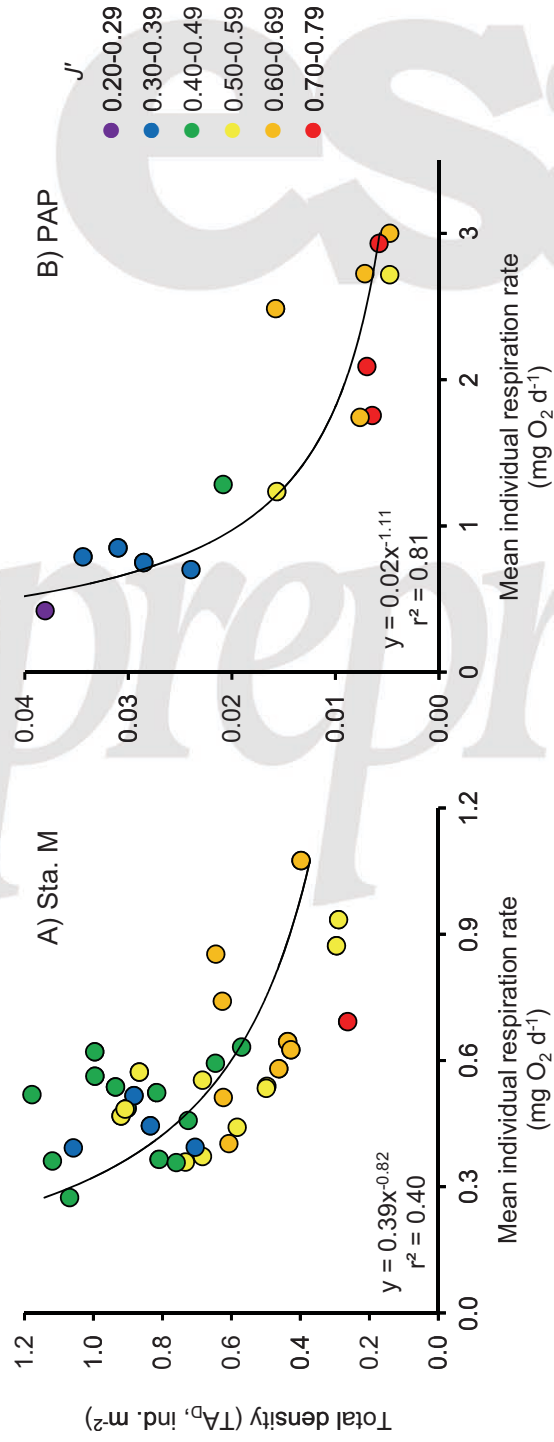
a

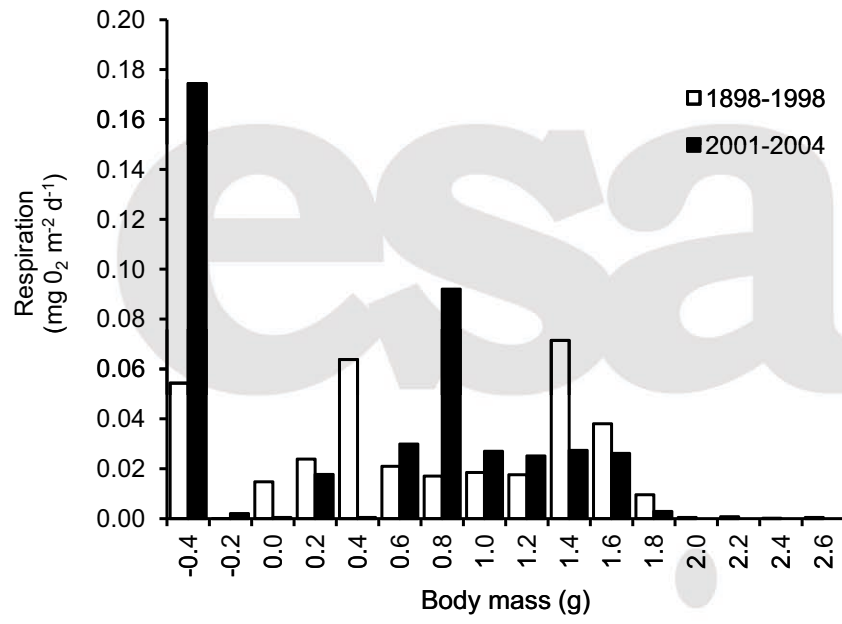
preprint











preprint

